

References and Notes

- (1) J. A. Laramée, P. H. Hemberger, and R. G. Cooks, *Int. J. Mass Spectrom. Ion Phys.*, **33**, 231 (1980).
- (2) E. Lindholm, *Adv. Chem. Ser.*, No. 58, 1 (1966).
- (3) T. Baer, A. S. Werner, B. P. Tsai, and S. F. Lin, *J. Chem. Phys.*, **61**, 5468 (1974).
- (4) D. M. Fedor and R. G. Cooks, *Anal. Chem.*, **52**, 679 (1980).
- (5) J. A. Laramée, P. H. Hemberger, and R. G. Cooks, *J. Am. Chem. Soc.*, **101**, 6460 (1979).
- (6) F. T. Smith, R. P. Marchi, and K. G. Dedrick, *Phys. Rev.*, **150**, 79 (1966).
- (7) Chr. M. Lehmann and G. Liebfried, *Z. Phys.*, **172**, 465 (1962).
- (8) F. T. Smith, R. P. Marchi, W. Aberth, D. C. Lorents, and O. Heinz, *Phys. Rev.*, **161**, 31 (1967).
- (9) (a) J. T. Park in "Collision Spectroscopy", R. G. Cooks, Ed., Plenum Press, New York, 1978; (b) M. S. Child, "Molecular Collision Theory", Academic Press, New York, 1974.
- (10) M. Barat, J. Baudon, M. Abignoli, and J. C. Houver, *J. Phys. B*, **3**, 230 (1970).
- (11) J. A. Laramée, J. J. Carmody, and R. G. Cooks, *Int. J. Mass Spectrom. Ion Phys.*, **31**, 333 (1979).
- (12) J. Baudon, M. Barat, and M. Abignoli, *J. Phys. B*, **3**, 207 (1970).
- (13) M. Vestal and G. Lerner, "Fundamental Studies Relating to the Radiation Chemistry of Small Organic Molecules", Office of Aerospace Research, USAF, ARC67-01114, 1067.
- (14) B. Andlauer and Ch. Ottinger, *J. Chem. Phys.*, **55**, 1471 (1971).
- (15) K. Levsen, "Fundamental Aspects of Organic Mass Spectrometry", Verlag Chemie, New York, 1978.
- (16) (a) F. W. McLafferty, "High Performance Mass Spectrometry: Chemical Applications", ACS Symposium Series 70, American Chemical Society, Washington, D.C.; (b) K. Levsen and H. Schwarz, *Angew. Chem., Int. Ed. Engl.*, **15**, 509 (1976); (c) T. L. Kruger, J. F. Litton, R. W. Kondrat, and R. G. Cooks, *Anal. Chem.*, **48**, 2113 (1976).
- (17) P. H. Hemberger, A. R. Hubik, J. A. Laramée, and R. G. Cooks, in preparation.

Effect of the Methyl Group Rotation on the Rate of Intramolecular Proton Exchange in α -Methyl- β -hydroxyacrolein

J. H. Busch, E. M. Fluder, and Jose R. de la Vega*

Contribution from the Chemistry Department, Villanova University, Villanova, Pennsylvania 19085. Received November 1, 1979

Abstract: Ab initio SCF calculations were used to determine the potential-energy profile for the intramolecular proton exchange in α -methyl- β -hydroxyacrolein for various orientations of the methyl group. The proton transfer was found to occur only when the methyl group orientation causes the transfer profile to be symmetric. Thus rotation and transfer were seen to be strongly coupled, in agreement with experimental evidence. An analytical two-dimensional potential representing the coupled motion was fitted to the SCF energies obtained. From the eigenstates of the potential the splitting of the two nondegenerate A levels and that of the lowest degenerate E levels were calculated and found in reasonable agreement with those estimated from experimental data.

Introduction

A mechanism involving tunnelling has been suggested to explain the very large value of the rate constant for the acid-base neutralization reaction in condensed phases of water and methyl alcohol.^{1,2} The tunnelling occurs when the proton moves from the donor to the acceptor site in a double minimum potential energy profile. Theoretical studies of the motion of the proton in this potential³⁻⁵ indicate that in symmetric profiles the rate of proton exchange is several orders of magnitude larger than that predicted from the semiclassical WKB approach which can be successfully used in asymmetric profiles and unbonded systems. Even though the calculated results in the cases of ice, liquid water, and methyl alcohol⁵ were consistent with the accepted experimental values, questions remain on the applicability of the calculation to condensed phases.

Interpretation of the microwave spectrum of the molecule of β -hydroxyacrolein⁶ suggests the existence of a long-amplitude nonharmonic oscillation due to the intramolecular hydrogen bonded proton exchange. In this case, the interaction between the proton exchange and the surrounding molecules is reduced to a minimum.

Experimentally⁷ and theoretically^{8,9} the geometry of minimum energy for the molecule corresponds to the asymmetric conformation with the proton covalently bound to either one of the oxygens. The energy for the geometrically optimized symmetric intermediate is calculated to be 11.6 kcal/mol above the minima.⁹ The reaction coordinate for the interconversion of the two equivalent minimum energy conformations is a symmetric double minimum energy potential. Theoretical calculations for the proton exchange in this case⁹ resulted in

a tunnelling frequency that was within the range of values deduced from the interpretation of the microwave spectrum.

Substituted β -hydroxyacrolein molecules may provide an opportunity to study the role of the symmetry of the profile in proton-exchange mechanisms. α -Methyl- β -hydroxyacrolein is the simplest of these substituted molecules for which reliable theoretical calculations are feasible.

In this molecule, the double-minimum potential for the proton exchange will be symmetric only when one of the C-H bonds of the methyl group is in a plane that is perpendicular to the plane containing all the carbon and oxygen atoms of the molecule. Departure from this geometry by rotation of the methyl group will result in an asymmetric double minimum profile. This asymmetry may reduce or completely eliminate tunnelling. As a result tunnelling will only occur at selected conformations of the methyl group, in which case a very strong coupling between the two motions will result. This coupling has been suggested by Sanders^{10,11} from a study of the microwave spectrum of the molecule.

Calculations

Ab initio, self-consistent-field calculations with an extended basis set known as 4-31G^{12,13} were performed to determine the energy of the five significant geometries of the molecule of α -methyl- β -hydroxyacrolein. These five geometries are represented by structures I-V in Figures 1 and 2. For each of the five geometries the bond lengths and the bond angles were varied until the minimum energy was achieved. These bond lengths and angles are shown in Tables I and II. The numbers

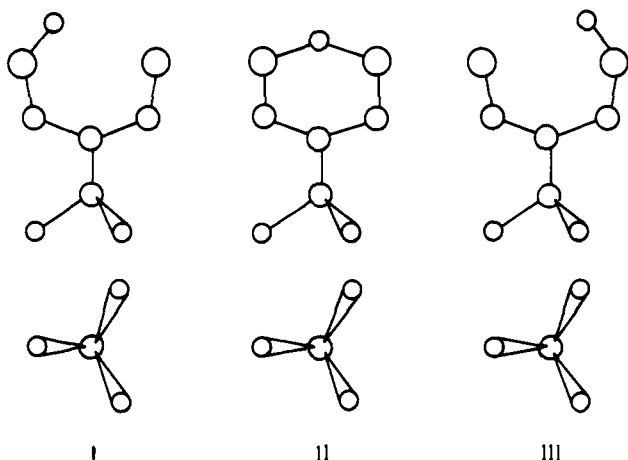


Figure 1. Schematic representation of geometries I, II, and III for H transfer without rotation, resulting in an asymmetric energy profile; atoms are identified in Figure 3 and parameters listed in Tables I and II.

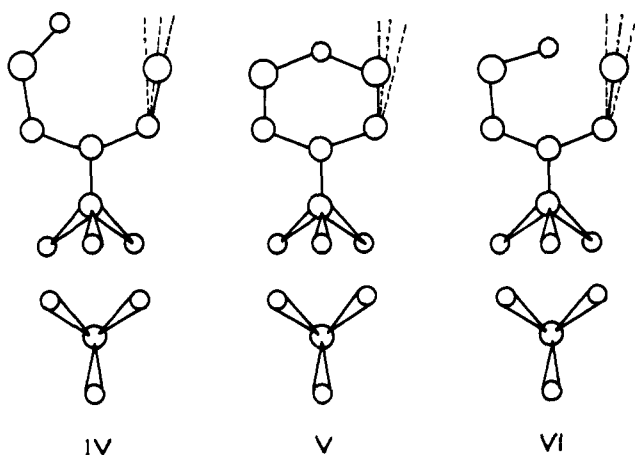


Figure 2. Structure IV represents the initial and final geometry for H transfer without rotation; structure V represents the intermediate geometry in this transfer for which the energy profile is symmetric. Structure VI represents the intermediate with all carbon and oxygen atoms in positions average between their initial and final ones, and the exchange proton in the position of minimal energy along the bisector of angle $C_2C_3C_4$.

assigned to identify each of the atoms in the molecule are given in Figure 3. It follows from the results obtained that only the bond lengths and angles involving the two oxygens and intervening hydrogen change significantly during the process of proton exchange. The C-H bond lengths and angles do not change appreciably during the process. It is also evident that, as the methyl group rotates, the methyl C-H bonds and angles remain practically constant.

The geometry of minimum energy is represented by structure I in which the O-H bond and one of the C-H bonds of the methyl group are in the same plane and in cis position. In structure III, the O-H bond and the methyl C-H bond are in the same plane too, but in position trans. The energy for this structure is 1.709×10^{-3} au higher than that of structure I. Interconversion of the two structures with structure II as an intermediate produces an asymmetric double minimum potential with a barrier of 0.0187 au. For this exchange, the conformation of the methyl group remains unchanged. With this profile^{2,3} the proton will remain localized at the position of minimum energy (no tunnelling).

The profile for the exchange of the hydrogen-bonded proton will be symmetric only when the methyl group is at the 30° position (structures IV and V) where one of the methyl C-H bonds is in a plane perpendicular to the plane of the oxygen and carbon atoms. This indicates that the hydrogen-bonded proton will tunnel only when one of the C-H bonds of the methyl

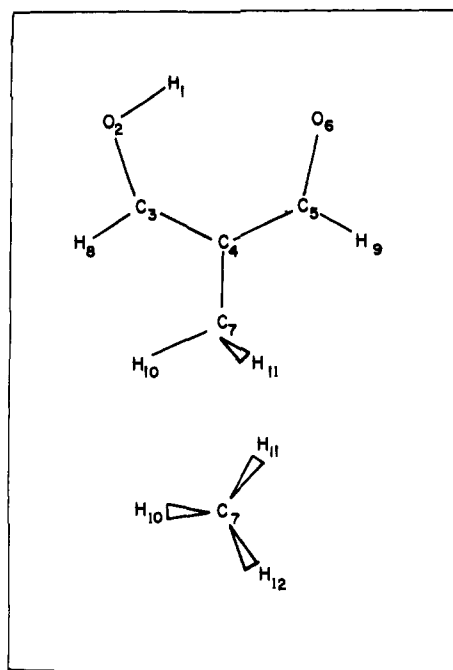


Figure 3. The diagrams identify the atoms with the numbers by which they are referred to in the text and in Tables I and II.

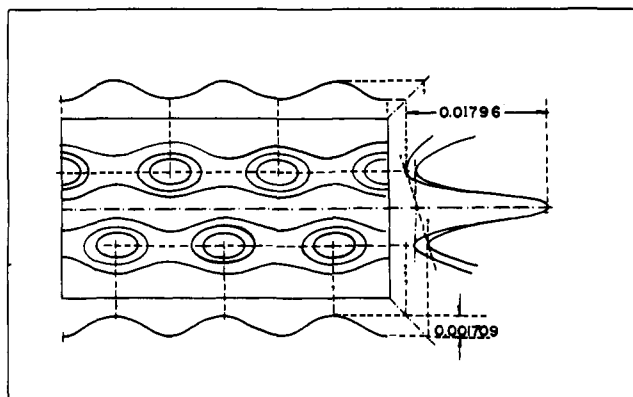


Figure 4. Sketch of contours in the two-dimensional potential energy surface defined by eq 1. The horizontal coordinate represents the angle θ , the vertical the reaction coordinate for the exchange.

group is in a plane perpendicular to the plane of the molecule containing the carbon and oxygen atoms. This requirement couples the motion of the methyl group with the proton exchange. The potential energy for this motion is a function of two variables, the reaction coordinate along which the system moves when the proton exchanges and θ , the angle of rotation of the methyl group.

In order to find the function that properly represents this potential, the rotation of the methyl group is studied at two positions of the intervening proton: in structures II and V the proton is kept at the position of maximum energy along the reaction coordinate. The rotation of the methyl group, which has a sixfold symmetry profile, has such a small barrier (1×10^{-5} au) that it could be considered free. From structures I and III it follows that, when the proton is at its position of minimum energy, the rotation, which now has a threefold symmetry, has a barrier of 1.709×10^{-3} au. This result indicates that the barrier for the rotation increases with χ , the distance along the reaction coordinate of the proton from its position at the center. Thus, eq 1 is a proper functional representation for the two-dimensional potential represented graphically in Figure 4:

$$V(x) + (v_3/2)(x_0 - x \cos 3\theta) \quad (1)$$

Table I. Bond Distances (Å) of the Five Structures Depicted in Figures 1 and 2^a

bond	structure					
	I	II	III	IV	V	VI
H(1)-O(2)	0.964	1.191	1.845	1.964	1.191	1.404
H(1)-O(6)	1.845	1.191	1.964	1.845	1.191	1.404
O(2)-C(3)	1.336	1.383	1.240	1.336	1.383	1.288
C(3)-C(4)	1.347	1.390	1.456	1.347	1.390	1.402
C(4)-C(5)	1.456	1.390	1.347	1.456	1.390	1.402
C(5)-O(6)	1.240	1.283	1.336	1.240	1.283	1.288
C(4)-C(7)	1.509	1.505	1.514	1.511	1.505	1.512
C(3)-H(8)	1.090	1.090	1.090	1.090	1.090	1.090
C(5)-H(9)	1.090	1.090	1.090	1.090	1.090	1.090
C(7)-H(10)	1.084	1.083	1.083	1.083	1.083	1.083
C(7)-H(11)	1.084	1.083	1.083	1.083	1.083	1.083
C(7)-H(12)	1.084	1.083	1.083	1.083	1.083	1.083
<i>E</i> + 304.	0.217 57	0.198 83	0.215 90	0.216 73	0.198 82	0.189 01

^a The numbers used to identify the atoms correspond to those shown in Figure 3. I and III are the geometrically optimized minimum energy structures. Within the constraints of the geometry, the bonds and angles of the remaining structures were changed until the minimum energy was achieved.

Table II. Bond Angles (Degrees) of the Five Structures Given in Figure 1^a

angle	structure					
	I	II	III	IV	V	VI
H(1)-O(2)-C(3)	113.4	106.8	101.99	113.4	106.8	107.7
H(1)-O(6)-C(5)	102.0	106.8	113.42	102.0	106.8	107.7
O(2)-C(3)-C(4)	124.4	121.5	123.2	124.4	121.5	123.8
C(3)-C(4)-C(5)	120.8	114.8	120.8	120.8	114.8	120.8
C(4)-C(5)-O(6)	123.2	121.5	124.4	123.2	121.5	123.8
C(3)-C(4)-C(7)	119.6	122.6	119.6	119.6	122.6	119.6
O(2)-C(3)-H(8)	118.4	119.25	117.8	118.4	119.25	118.1
C(4)-C(5)-H(9)	117.8	119.25	118.4	117.8	119.25	118.1
C(4)-C(7)-H(10)	111.4	111.42	111.54	111.47	111.42	111.5
C(4)-C(7)-H(11)	111.4	111.42	111.54	111.47	111.42	111.5
C(4)-C(7)-H(12)	111.4	111.42	111.54	111.47	111.42	111.5
H(10)-C(7)-H(11)	107.5	107.46	107.33	107.40	107.46	107.4

^a The numbers used to identify the atoms are those shown in Figure 2.

$V(x)$ is a symmetric double minimum potential that can be fitted to a parabola and a Gaussian, two Morse curves, or a fourth-degree polynomial, depending on the values of E , D , and k_m .⁹ v_3x_0 is the barrier for the rotation at $x = x_0$, the position of the minimum along the reaction coordinate for the exchange; θ is the angle of rotation referred to the position that the methyl group has in structures IV and V.

The complete Hamiltonian for this system is written as a sum of three terms. One, \mathcal{H}^0 , containing the reaction coordinate x , represents the motion of the proton in a symmetric double minimum potential. A second term, Λ_0 , contains the angle θ of rotation of the methyl group. The third term, given by eq 1, couples the two motions.

$$\mathcal{H} = \mathcal{H}^0 + \Lambda^0 + (v_3/2)(x_0 - x \cos 3\theta) \quad (2)$$

The eigenstates $\Phi_\mu(n, x)$ of \mathcal{H}^0 reflect the symmetry of the double-minimum potential where $V(x) = V(-x)$:

$$\mathcal{H}^0\Phi_\mu(n, x) = E_{\mu, n}\Phi_\mu(n, x) \quad (3)$$

The subscript μ indicates the symmetry species to which the eigenstate belongs. They are

$$\begin{aligned} \Phi_g(n, x) &= \Phi_g(n, -x) \\ \Phi_u(n, x) &= -\Phi_u(n, -x) \end{aligned} \quad (4)$$

The eigenfunctions $g(m, \theta)$ and eigenvalues E_m of the Hamiltonian Λ_0 are

$$\begin{aligned} g(m, \theta) &= (1/\sqrt{2\pi})e^{im\theta} \\ E_m &= (\hbar^2/2I)m^2 \end{aligned} \quad (5)$$

The eigenfunctions $\Psi(x, \theta)$ of the total Hamiltonian \mathcal{H} are calculated by the variational method using as basis set the eigenfunctions $\Phi_\mu(n, x)$ and $g(m, \theta)$ of the uncoupled Hamiltonian:

$$\Psi(x, \theta) = \frac{1}{\sqrt{2\pi}} \sum_{\mu=g}^u \sum_{n=0}^{\infty} \sum_{m=-\infty}^{\infty} C_{\mu}(n, m) \Phi_{\mu}(n, x) e^{im\theta} \quad (6)$$

In this representation the matrix elements of the Hamiltonian are

$$\begin{aligned} \langle \mu, n, m | \mathcal{H} | \mu', n', m' \rangle \\ = \langle \mu, n, m | \mathcal{H}^0 + \Lambda^0 + (v_3/2)x_0 | \mu', n', m' \rangle \\ + (v_3/2) \langle \mu, n, m | x \cos 3\theta | \mu', n', m' \rangle \end{aligned} \quad (7)$$

The first term in eq 7 represents the matrix elements of the uncoupled Hamiltonian that is diagonal in this representation. Its values are given by

$$\begin{aligned} \langle \mu, n, m | \mathcal{H}^0 + \Lambda^0 + (v_3/2)x_0 | \mu', n', m' \rangle \\ = (E_{\mu, n} + (\hbar^2/2I)m^2 + (v_3/2)x_0) \delta_{\mu, \mu'} \delta_{n, n'} \delta_{m, m'} \end{aligned} \quad (8)$$

They are the energy levels for the proton in a symmetric double minimum potential to which the energy levels $F_{\mu, n}$ of the free rotor E_m have been added. The second term in the equation is equal to

$$\begin{aligned} (v_3/2) \langle \mu, n, m | x \cos 3\theta | \mu', n', m' \rangle \\ = (v_3/2) \langle \Phi_g(n, x) | x | \Phi_u(n', x) \rangle [\delta_{m, m+3} + \delta_{m, m-3}] \end{aligned} \quad (9)$$

This nondiagonal contribution mixes the rotational levels m and $m + 3$ as expected in a threefold restricted rotor. As shown in eq 9 the energy levels mixed must have different symmetry

Table III. Energy Splitting (MHz) between the E levels and A Levels for the Normal (H) and Deuterated (D) Species^a

	exptl	direct transfer	reaction coordinate transfer
M_h		1.097	4.289
M_D		2.095	5.071
d_0		1.664	1.930
E		0.0286	0.0179
V_3		0.001 709	0.001 709
(H) $A_{1g} A_{2u}$	84 012	37 677	219.9
(H) $E_u E_g$	41 200	18 840	108.30
(D) $A_{1g} A_{2u}$	10 776	1943.1	59.4
(D) $E_u E_g$	5383	940.5	29.4

^a The effective masses M are in amu. d_0 is the unit of length, in au, along the reaction path. E is the barrier for the double-minimum potential in au and V_3 is the torsional barrier in au.

with respect to the variable x . The matrix of \mathcal{H} can be reduced to six tridiagonal matrices, each belonging to a particular symmetry species of the group D_{3d} to which the Hamiltonian of the system belongs. The proper combination of basis functions can be found by writing the running index m as $6j + k$ where k goes from 0 to 5.

$$\Psi(x, \theta) = \frac{1}{\sqrt{2\pi}} \times \sum_{\mu=g}^u \sum_{n=0}^{\infty} \sum_{k=0}^5 \sum_{j=-\infty}^{\infty} C_{\mu}(n, k, j) \Phi_{\mu}(n, x) e^{i(6j+k)\theta} \quad (10)$$

The first of the six matrices is obtained by combining the $\Phi_g(n, x)$ with $k = 0$ and the $\Phi_u(n, x)$ with $k = 3$

$$\frac{1}{\sqrt{2\pi}} \sum_{n=0}^{\infty} \sum_{j=-\infty}^{\infty} \{C_g(n, 0, j) \Phi_g(n, x) e^{i(6j)\theta} + C_u(n, 3, j) \Phi_u(n, x) e^{i(6j+3)\theta}\} \quad (11)$$

The coefficients in eq 11 have the property

$$C_{\mu}(n, k, j) = \pm C_{\mu}(n, k, -j) \quad (12)$$

The plus or minus sign produces functions that remain unchanged or change sign with the symmetry operations that reverse the sign of θ (C_2 and σ_v of the group D_{3d}). Substitution of eq 12 in eq 11 produces the functions with A_{1g} and A_{2g} symmetry.

$$\Psi(A_{1g}) = \frac{2}{\sqrt{2\pi}} \sum_{n=0}^{\infty} \sum_{j=0}^{\infty} \{C_g(n, 0, j) \Phi_g(n, x) \cos(6j)\theta + C_u(n, 3, j) \Phi_u(n, x) \cos(6j + 3)\theta\} \quad (13)$$

$$\Psi(A_{2g}) = \frac{2i}{\sqrt{2\pi}} \sum_{n=0}^{\infty} \sum_{j=0}^{\infty} \{C_g'(n, 0, j) \Phi_g(n, x) \sin(6j)\theta + C_u(n, 3, j) \Phi_u(n, x) \sin(6j + 3)\theta\}$$

The combination of the Φ_u with $k = 0$ and the Φ_g with $k = 3$ produces the second of the six three-diagonal matrices. This matrix with the use of eq 12 gives the A_{1u} and A_{2u} symmetry species.

$$\Psi(A_{2u}) = \frac{2}{\sqrt{2\pi}} \sum_{n=0}^{\infty} \sum_{j=0}^{\infty} \{C_g(n, 3, j) \Phi_g(n, x) \cos(6j + 3)\theta + C_u(n, 0, j) \Phi_u(n, x) \cos(6j)\theta\} \quad (14)$$

$$\Psi(A_{1u}) = \frac{2i}{\sqrt{2\pi}} \sum_{n=0}^{\infty} \sum_{j=0}^{\infty} \{C_g'(n, 3, j) \Phi_g(n, x) \sin(6j + 3)\theta + C_u'(n, 0, j) \Phi_u(n, x) \sin(6j)\theta\} \quad (15)$$

Two of the remaining four matrices, corresponding to $k = 2, 4$ (or ± 2), combined with $\Phi_g(n, x)$, and $k = 1, 5$ (or ± 1) combined with $\Phi_u(n, x)$ will produce the two-dimensional ir-

Table IV. Rotational Constants for the Various Structures Depicted in Figures 1 and 2 and Tables I and II^a

	rotational constants, MHz		
	A	B	C
I	4885.35	3524.29	2073.17
II	5791.46	3520.18	2218.99
III	4885.35	3524.29	2073.17
IV	5791.46	3528.79	2182.33
V	4885.35	3524.29	2073.17
VI	4890.47	3527.94	2074.57
exptl	5029.28	3408.34	2094.15

^a The three rotational constants are calculated from the moments obtained by diagonalization of the moment of inertia tensor.

reducible representation E_g while the two other matrices combine $k = \pm 2$ with the $\Phi_u(n, x)$ and $k = \pm 1$ with the $\Phi_g(n, x)$ to give the two-dimensional irreducible representation E_u :

$$\Psi(E_g) = \frac{1}{\sqrt{2\pi}} \sum_{n=0}^{\infty} \sum_{j=-\infty}^{\infty} \{C_g(n, \pm 2, j) \Phi_g(n, x) e^{i(6j\pm 2)\theta} + C_u(n, \pm 1, j) \Phi_u(n, x) e^{i(6j\pm 1)\theta}\} \quad (16)$$

$$\Psi(E_u) = \frac{1}{\sqrt{2\pi}} \sum_{n=0}^{\infty} \sum_{j=-\infty}^{\infty} \{C_u(n, \pm 2, j) \Phi_u(n, x) e^{i(6j\pm 2)\theta} + C_g(n, \pm 1, j) \Phi_g(n, x) e^{i(6j\pm 1)\theta}\} \quad (17)$$

Results and Discussion

Two double-minimum profiles were used to calculate the parameters needed to determine the potential function $V(x)$ in eq 1. In one, the system moves along the reaction coordinate. The initial state corresponds to the asymmetric, geometrically optimized, minimum energy structure I. The symmetric intermediate corresponds to structure II. The motion of the system along the path of minimum energy involves appreciable displacement of the heavy atoms, especially the oxygens. As a result, a large value¹⁶ of the effective mass is obtained. This mass, together with the parameter v_3 needed in eq 1, is given in Table III. The splittings found for the lower nondegenerate A levels and the lower degenerate E levels are much lower than those predicted from the microwave data.

In the second double minimum profile, referred to as direct transfer, the initial state corresponds to the minimum energy structure VI (Figure 2 and Tables I and II). In this structure, the heavy atoms are in positions which are averages between the initial and final states. The position of the hydrogen-bonded proton is that of minimum energy along the bisector of angle C(3)-C(4)-C(5). For this profile the displacement of the heavy atoms is minimal and as a result an effective mass of 1.097 amu is obtained for the normal isotopic species and of 2.095 amu for the deuterated species. The calculated separations for the two lowest nondegenerate A levels and the two lowest degenerate E levels are roughly one-half of the estimated values obtained from the interpretation of the spectrum. The order of the levels, A_{1g} , E_u , E_g , and A_{2u} , agrees with that proposed by Wilson and Sanders.¹⁰

The values of the splitting for the deuterated species are approximately 5% (Table III) of those for the normal isotopic species, while the experimentally estimated ratio is about 12%.

This indicates that the effective mass involved is slightly larger than that theoretically estimated. It should be noticed that a slightly smaller C(3)-C(4)-C(5) angle for the minimum energy structure I could produce the correct effective mass and interminimal distance. This observation is consistent with the difference between the theoretical and the experimental values of the rotational constant A (Table IV). Such a discrepancy

is not unusual when ab initio calculations which do not include d orbitals and configuration interaction are used.^{8b}

Conclusion

Both theoretically calculated and experimental results^{9,10} indicate that the rate of proton exchange in α -methyl- β -hydroxyacrolein is one order of magnitude smaller than that of β -hydroxyacrolein.^{6,9} This difference is due to the strong coupling that exists between the proton exchange and the rotation of the methyl group. The strong coupling is due to the fact that the proton will exchange only when the conformation of the methyl group leads to a symmetric double minimum profile. The same effect was proposed to explain the rate of proton transfer between methoxide and methyl alcohol and methyl alcohol and methyloxonium ion.⁵

Acknowledgment. The authors wish to thank Professor E. Bright Wilson for his very helpful discussions and for making the experimental results available, Dr. John Pople for his helpful discussion on the symmetry, and Villanova University and its Computer Center for their support.

References and Notes

- (1) E. F. Caldin, "Fast Reactions in Solutions", Blackwell, Oxford, 1964, p 268.
- (2) E. Grunwald, C. F. Jumper, and S. Meiboom, *J. Am. Chem. Soc.*, **84**, 4664 (1962).
- (3) J. Brickmann and H. Zimmerman, *J. Chem. Phys.*, **50**, 1608 (1969).
- (4) M. C. Flanagan and J. R. de la Vega, *J. Chem. Phys.*, **61**, 1882 (1974).
- (5) J. H. Busch and J. R. de la Vega, *J. Am. Chem. Soc.*, **99**, 2397 (1977).
- (6) W. F. Rowe, R. W. Duerst, and E. B. Wilson, *J. Am. Chem. Soc.*, **98**, 4021 (1976).
- (7) (a) R. S. Brown, *J. Am. Chem. Soc.*, **99**, 5497 (1977); (b) R. S. Brown, A. Tse, T. Nakashima, and R. C. Haddon, *ibid.*, **101**, 3157 (1979).
- (8) (a) C. Karlstrom, H. Wennerstrom, B. Jonsson, S. Foren, J. Almlof, and B. Roos, *J. Am. Chem. Soc.*, **97**, 4188 (1975); (b) C. Karlstrom, B. Jonsson, B. Roos, and H. Wennerstrom, **98**, 6851 (1976).
- (9) E. M. Fluder and J. R. de la Vega, *J. Am. Chem. Soc.*, **100**, 5265 (1978).
- (10) E. B. Wilson, private communication.
- (11) N. D. Sanders, Doctoral Thesis, Harvard University, June 1979.
- (12) W. J. Hehre, R. F. Stewart, and J. A. Pople, *J. Chem. Phys.*, **51**, 2657 (1969).
- (13) R. Ditchfield, W. J. Hehre, and J. A. Pople, *J. Chem. Phys.*, **54**, 724 (1971).
- (14) R. A. Marcus, *J. Chem. Phys.*, **41**, 2624 (1964).
- (15) E. M. Fluder and J. R. de la Vega, *Chem. Phys. Lett.*, **59**, 454 (1978).
- (16) The effective mass was calculated as the ratio of the component along the reaction coordinate g_{rr} of the kinetic energy tensor to the metric g_{rr} .¹⁴ The average values for $(\partial x_i / \partial \xi)^2$ were calculated from the initial and intermediate structures after elimination of translational and rotational displacements.

A Predictor of Reactivity in Allowed Photodimerizations and Photocycloadditions

Richard A. Caldwell

Contribution from the IBM Research Laboratory, San Jose, California 95193, and the Department of Chemistry,[†] The University of Texas at Dallas, Richardson, Texas 75080. Received July 30, 1979

Abstract: A paradigm for prediction of reactivity in allowed, [2 + 2] and [4 + 4] singlet-state photodimerizations and photocycloadditions is developed and compared to results obtained from the literature. Favorable features for high reactivity are high singlet energy, low triplet energy, and high frontier orbital density at reacting positions. The quantitative algorithm $\gamma(r_c) = (E_T^A + E_T^B - E_S^A)/c^2$ is derived, where $\gamma(r_c)$ is the resonance integral for end-on interaction of carbon 2p orbitals at distance r_c , E_T^A and E_T^B are triplet energies of reactants A and B, E_S^A is the singlet energy of the excited reactant A, and c^2 is the sum of HOMO and LUMO orbital coefficient products over reacting positions. The algorithm correlates a substantial body of known photoreactivities with considerable success.

Despite the large number of allowed, [2 + 2] and [4 + 4] singlet-state photocycloadditions and photodimerizations reported in the last 15 years,¹ a simple paradigm for predicting reactivity has not hitherto emerged. Some theoretical treatments have offered elegant but qualitative analyses based on state correlation diagrams; cf. especially the analysis of the $H_2 + H_2$ reaction by Michl and co-workers.² Others³ have emphasized PMO techniques,^{3a} frontier orbitals,^{3b} or configuration interaction analysis.^{3c} The Michl model has been useful both to others^{4,5} and to us⁶ in rationalizing certain aspects of photocycloaddition reactivity. Further tests of the model would increase our confidence in its utility and, if quantitative, might lead to a generally useful structure-reactivity relationship.

The analysis below suggests and tests a paradigm based on the Michl model which places [2 + 2] and [4 + 4] singlet-state photodimerizations and photocycloadditions on a common scale. Favorable features for high reactivity are high singlet energy, low triplet energy, and high frontier orbital density at reacting positions. An easily applied algorithm allows concrete predictions of reactivity.

The Model

The feature of allowed photocycloadditions key to the present analysis is the correlation of a doubly excited configuration D of addends with the ground state $G^{2,6}$ of the adduct. The crossing of this correlation line with the S-S line essentially locates the transition state for the reaction (Figure 1). Note that the point at which crossing occurs would be determined if the D-S gap at infinite separation ΔE_∞ and the behavior of the two correlation lines up to the crossing point were known.

The D-S gap ΔE_∞ is usually known precisely! The D state in this region in fact corresponds to overall singlet coupling of the HOMO-LUMO (i.e., L_a) triplets of the reacting partners.² For common chromophores, this is nearly always the lowest triplet, for which triplet energies are generally available. The S state corresponds to excitation of the reactant of lower excitation energy. For reactants A and B, then, with $E_S^A < E_S^B$, ΔE_∞ may be expressed as

$$\Delta E_\infty = E_T^A + E_T^B - E_S^A \quad (1)$$

As reaction proceeds, the D state drops extremely rapidly as a result of the interchromophoric interaction. The initial

[†] Permanent address.